

Influence of step and island edges on local adsorption properties: Hydrogen adsorption on Pt monolayer island modified Ru(0001) electrodes

Sung Sakong · Julia M. Fischer · David
Mahlberg · R. Jürgen Behm · Axel Groß

accepted: 18 January 2017

Abstract The influence of steps and island edges on the local electronic structure of a (bi-)metallic single crystalline electrode surface and on the local, site specific adsorption energy of adsorbed species, so-called structural effects, was studied by periodic density functional theory based calculations, focusing on longer-range effects. Using hydrogen adsorption energies as a local probe, calculations were performed both for partly Pt monolayer covered planar Ru(0001) surfaces and for a stepped Ru(10 $\bar{1}$ 9) surface decorated with a row of Pt atoms. The calculations demonstrate that the steps / island edges affect not only the nearest neighbor adsorption sites, but also more distant ones with the extent depending on the particular structure. This longer-range effect is in excellent agreement with recent temperature programmed desorption and spectroscopy experiments (H. Hartmann et al., Phys. Chem. Chem. Phys. 14, (2012) 10919). For the interaction of water molecules with partly Pt monolayer covered Ru(0001), similar trends as in the hydrogen adsorption have been found. In addition, hydrogen adsorption energies as a function of coverage have been used to derive the hydrogen coverage as a function of the electrorode potential, exhibiting a broad range of stable hydrogen adsorption structures.

Keywords Adsorption, step, bimetallic catalysts, site selective adsorption, density functional calculations, PtRu, hydrogen, water

The final publication is available at Springer via <http://dx.doi.org/10.1007/s12678-017-0354-1>

Sung Sakong
Institute of Theoretical Chemistry, Ulm University, 89069 Ulm, Germany

Julia M. Fischer
Australian Institute for Bioengineering and Nanotechnology, The University of Queensland,
St Lucia QLD 4072, Australia

David Mahlberg
Institute of Theoretical Chemistry, Ulm University, 89069 Ulm, Germany

R. Jürgen Behm
Institute of Surface Chemistry and Catalysis, Ulm University, 89069 Ulm, Germany

Axel Groß
Institute of Theoretical Chemistry, Ulm University, 89069 Ulm, Germany

1 Introduction

It is well known from both experiment and theory that steps, and in a more general picture, undercoordinated sites cause a distinct modification in the interaction between metal surfaces and adsorbed species. Even for apparently well prepared single-crystal surfaces and electrodes experimental studies often reveal deviations from the expected energetics, such as a broadening of peaks or even the presence of additional states, e.g., in thermal desorption spectroscopy (characterization under ultrahigh (UHV) vacuum conditions) or in cyclic voltammetry (characterization of the electrochemical properties). Early examples are, e.g., the adsorption of hydrogen on Pt(111), where a distinct feature at the high temperature side of the H₂ desorption peak was attributed to desorption from step sites [1,2]. Likewise, numerous quantum chemical calculations based on density functional theory (DFT) have shown an increase of the binding energy for adsorption on step atoms at the upper terrace side of the steps [3–5]. Utilizing the d-band model developed by Hammer and Nørskov [6], this can be explained by an up-shift of the center of the d-band in the projected density of states on these step edge surface atoms caused by their lower coordination. The role of steps and other defects was particularly discussed in the context of catalytic reactions, where these were often considered as active sites [7]. A prominent example is the dissociative adsorption of nitrogen on Ru(0001) as rate limiting step in the ammonia synthesis reaction, where the presence of steps was demonstrated to raise the rate for dissociative adsorption of N₂ by more than six orders of magnitude [8]. Another prominent example is the facile dissociation of O₂ on stepped Pt surfaces [4,9,10]. In electrocatalysis, the presence of steps can also modify the catalytic activity significantly. For example, it was shown [11] that increasing the surface step density of Pt electrodes increases the activity of the electrode with respect to the oxygen reduction reaction (ORR). At least qualitatively such effects can be rationalized by a lowering of reaction barriers at steps [8].

While there is general agreement that steps and defects modify the structural, electronic, and chemical properties of these sites, much less is known on the range of these effects. In the experimental studies, the concentration of defects was mostly not sufficiently well defined for a quantitative evaluation, and in most calculations, only adsorption on the outermost adsorption sites was considered. Furthermore, the difference in adsorption energies was often not large enough that desorption from different sites could be separated quantitatively. On the other hand, assuming a Friedel-type behavior, one would expect that the step induced modification of the adsorption energy is longer-range, but decreases with increasing lateral distance from the step, possibly in an oscillatory behavior. In a recent temperature programmed desorption (TPD) study on the effect of Pt monolayer islands on the adsorption of CO and hydrogen on partly Pt monolayer covered Ru(0001) surfaces [12], we observed that i) in addition to desorption from bare Ru(0001) and from Pt monolayer island covered areas there is also significant desorption in between the states related to desorption from the above areas, and that ii) the intensity in the additional state was too much to be explained by desorption from sites directly located at the terrace or island edges only. First results in that direction were also obtained for electrode reactions, under electrochemical conditions. Studying hydrogen adsorption [13,14] and the H₂ evolution reaction [15] on vicinal Ag(11n) electrodes, Santos and coworkers derived from density functional theory

(DFT) based calculations that both adsorption energies and H_2 evolution rates varied with the distance from the step edge.

Such effects are background of the present work, which, following the experimental work mentioned above, aims at a detailed atomic scale understanding of the impact of steps and island edges on the interaction of hydrogen with a Ru(0001) surface partly modified by monolayer Pt islands ($Pt_{0.x-ML}/Ru(0001)$) which we will denote in short as Pt/Ru surfaces. In order to test the hypothesis of longer-range effects at island edges and steps, we systematically investigated the local electronic structure as well as the local hydrogen chemisorption properties along the edge of a Pt monolayer island on Ru(0001) as a function of distance from the edge, both on the bare Ru(0001) side of the edge and on the Pt monolayer island, employing periodic DFT based calculations. These calculations were performed on a partly Pt covered smooth Ru(0001) surface and on a stepped Ru(10 $\bar{1}$ 9) surface with the steps decorated by one row of Pt atoms, to address also the influence of substrate steps. In order to test not only for the modification of the adsorption energy of individual (separated) H adatoms, but be closer to a TPD experiment, we also calculated the effect of higher H_{ad} coverages on the differential adsorption energy. This includes contributions from interactions between adsorbed H_{ad} species.

In the following, we will, after a brief description of the calculational details, first briefly summarize the main results of our previous experimental study relevant for this study. Subsequently we present and discuss results on the modifications in the electronic structure of the surface in the vicinity of the Pt island edge, both on Ru(0001) and on the stepped Ru(10 $\bar{1}$ 9) surface. Next we will evaluate the local hydrogen adsorption energy of individual hydrogen species at a variety of different sites at different distances from the island edges, varying also the width of the Pt monolayer islands. Subsequently, we will assess the role of H_{ad} - H_{ad} interaction in calculations performed at higher H_{ad} coverages, to better mimic the situation during temperature-programmed desorption (TPD) experiments. Finally, the main findings from this work will be summarized.

2 Computational Details

Periodic DFT calculations have been performed using the Vienna ab initio software package (VASP) [16]. The electronic cores are described by the projector augmented wave method [17] and the electronic one-particle states in the water-metal calculations have been expanded up to 400 eV using a plane wave basis set. In order to describe exchange-correlation effects, the generalized gradient approximation (GGA) using the Perdew-Burke-Ernzerhof (PBE) functional [18] has been employed. Thus the results of these calculations can be compared with previous studies in our group addressing hydrogen adsorption on metal electrodes [19]. The resulting optimized Ru lattice parameters are $a = 2.71 \text{ \AA}$ and $c/a = 1.58$.

The metal electrodes were modeled by five-layer slabs which were separated by a vacuum layer of 15 \AA . The top three layers of the slabs were fully relaxed, while the bottom two layers were fixed at their bulk positions. Pt islands on Ru(0001) are modeled within a (8×2) geometry using a k -point sampling of $2 \times 8 \times 1$ to replace the integration over the first Brillouin zone. Ru steps were modeled by a Ru(10 $\bar{1}$ 9) slab within a (1×2) geometry that exhibits both (111)-like and (100)-like

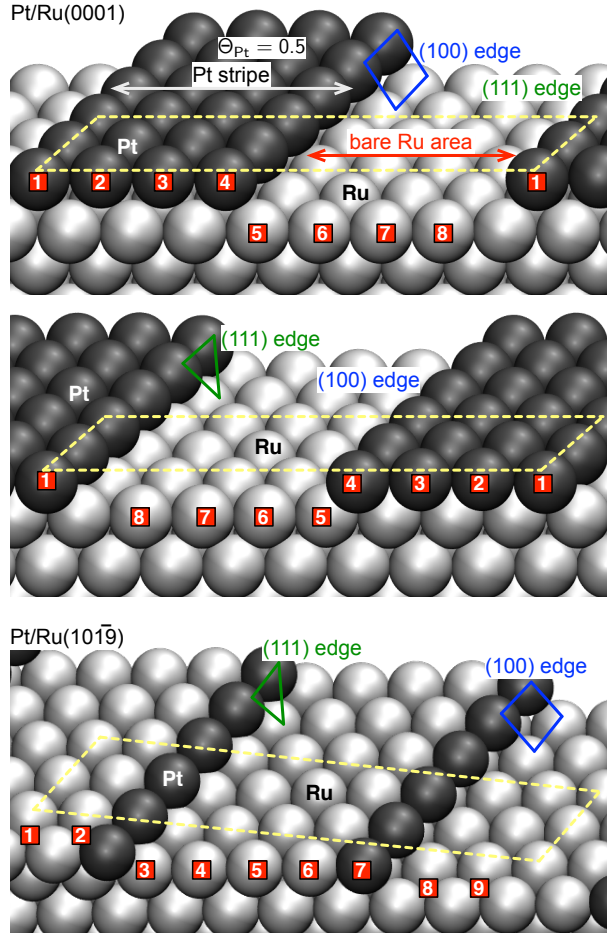


Fig. 1 Geometric arrangement to model Pt islands on Ru(0001) employing 8×2 surface unit cells. As an example, Pt islands consisting of four atomic rows are plotted in top and middle panels. Note that on hexagonal close-packed surfaces, straight islands are bounded by two different kind of steps with either a square (100)-like structure or a triangular (111)-like arrangement which is illustrated in the two upper panels that show the same surface just rotated around the surface normal by 180° . The bottom panel shows Pt-decorated Ru steps modeled by a Ru(101̄9) surface with one row of Pt atoms attached to the steps.

step edges, and a row of Pt atoms is attached to both kinds of steps, as illustrated in the bottom panel of Fig. 1.

Hydrogen adsorption energies per hydrogen atom for n hydrogen atoms per surface unit cell were determined with respect to the free H_2 molecule according to

$$E_{n\text{H}_{\text{ad}}} = \left(E_{n\text{H}/\text{electrode}} - E_{\text{electrode}} - \frac{n}{2} E_{\text{H}_2} \right) / n, \quad (1)$$

where $E_{n\text{H}/\text{electrode}}$ is the total energy per unit cell of the Pt/Ru electrode with n adsorbed hydrogen atoms, and $E_{\text{electrode}}$ and E_{H_2} are the total energies of the

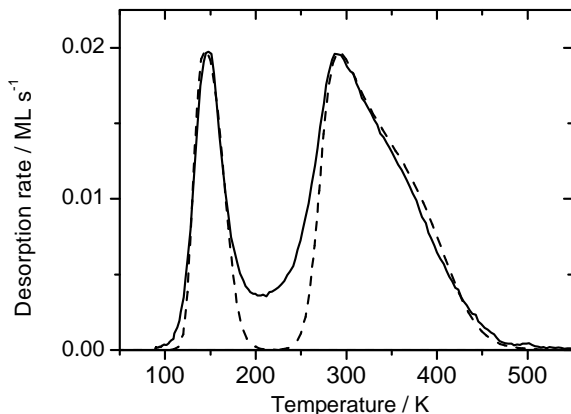


Fig. 2 Experimental TPD spectrum recorded after a D_2 exposure of 10×10^{-6} mbar-s to a bimetallic Pt/Ru(0001) surfaces with 0.5 ML Pt monolayer islands (full line) and simulated spectrum based on a numerical solution of the rate equations (Polanyi-Wigner equations) for second order recombinative deuterium desorption using standard parameters (dashed line) (adapted from Ref. [12]).

clean Pt/Ru electrode within the same unit cell and of the free H_2 molecule, respectively.

3 Results and Discussion

3.1 Experimental observations

First we briefly summarize the experimental observations that have already been reported before [12].

Investigating the adsorption of hydrogen and CO on a Ru(0001) partly covered by Pt monolayer islands we recently found that desorption of hydrogen adsorbed on the Pt monolayer islands is well separated from desorption from Ru(0001) substrate areas, with the former one occurring in a peak centered at about 140 K (γ_1 -peak), while the latter gives rise to a desorption peak ranging from 260 to 450 K at saturation [12]. This is illustrated in Fig. 2 in TPD spectra recorded for deuterium desorption from partly Pt monolayer island covered Ru(0001) surfaces (0.5 monolayers (ML) Pt, D_{ad} saturation). Hence, one would expect that for a surface partly covered by Pt monolayer islands the respective desorption peaks are well separated, as they appear in numerical simulations using desorption parameters typical for these two adsorption states [12]. Experimentally, however, one finds that there is significant desorption intensity in the temperature range between the two peaks, even for optimized, defect free surfaces. Qualitatively, desorption in this temperature range can be explained by desorption from more strongly binding adsorption sites along the Pt island edge or from less strongly adsorbing sites along the Pt island edges on the Ru terrace side. Quantitatively, however, the fraction of these sites was far too low to explain the observed intensity, considering

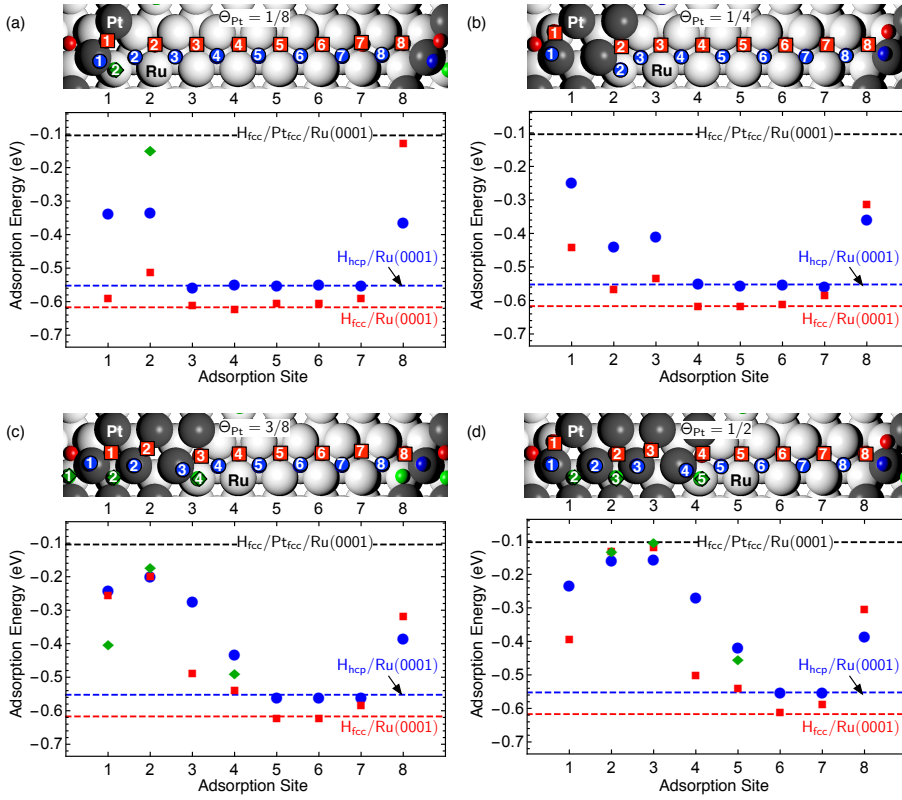


Fig. 3 Adsorption energy of isolated hydrogen atoms on Pt/Ru(0001) surfaces within a (8×2) geometry with Pt islands consisting of one to four atomic rows. The numbering of the atomic positions is illustrated in the panels above the diagrams. The dashed lines denote the hydrogen adsorption energies at the fcc site on a flat Pt monolayer on Ru(0001) and at the hcp and fcc sites of Ru(0001), respectively.

that the Pt islands on this surface, which were prepared by Pt evaporation on the substrate at 300 K sample temperature and subsequent annealing at 700 K for 60 s, have typical diameters of 10–20 nm. Even when assuming that in addition to the stronger adsorption on Pt island edge sites there is also weaker adsorption on the Ru side of the island edges, which would also contribute to the intensity between the two desorption peaks, this would still not be sufficient to match the experimentally observed intensity between the two desorption peaks. In order to rationalize the observed desorption intensity between the two H_2 desorption peaks, one would have to assume that the Pt island edge modifies the binding energy of at least two rows of H adatoms along the island edge on each side of the step [12]. This is the hypothesis which shall be tested and verified in the following.

3.2 Adsorption of single hydrogen atoms

The adsorption of hydrogen on Pt/Ru(0001) bimetallic surfaces was investigated in a series of calculations within a (8×2) geometry. The Pt islands on Ru(0001) were modeled by pseudomorphic one-dimensional strings, whose width was varied from 1 to 4 atomic Pt rows, whereas they extend infinitely in the other direction. This results in a width of the Pt-free Ru(0001) surface area of between 7 and 4 Ru surface atoms, which is illustrated in Fig. 1a and in the upper panels of Fig. 3.

The adsorption energies $E_{\text{H}_{\text{ad}}}$ on the Pt/Ru(0001) electrodes with Pt islands that are one to four atomic rows wide are plotted in Fig. 3. All adsorption positions are fully relaxed. Initially the hydrogen atoms were placed either on the fcc or hcp threefold hollow sites on the Ru terrace or on the Pt island, or at highly coordinated sites at the island edge. In some cases, subsequent relaxation allowed them to move to the positions indicated in the figure. Note that the absolute values of the adsorption energies have the typical technical uncertainty of DFT results of about 0.1 eV on top of the uncertainty related to the choice of the functional. However, relative trends in the adsorption energies as a function of the adsorption site should be reliable to within 0.02 eV as they have been determined with the same technical setup.

First of all, it is obvious that hydrogen bonding on the Ru(0001) substrate is much stronger than on the Pt islands. This can be explained by the fact that Ru has a smaller d -band filling than Pt and is therefore more reactive. The fact that hydrogen bonding on the Pt islands is even weaker than on Pt(111) ($E_{\text{H}_{\text{ad}}} = -0.48$ eV [19]) has been demonstrated also experimentally [12]. The modification of adsorption energies on bimetallic overlayer systems is indeed well-understood [20–23]: Both the strong interaction of the underlying Ru substrate with the Pt surface atoms (“vertical electronic ligand effect”) as well as the compression of the pseudomorphic Pt layer with respect to bulk Pt caused by the smaller lattice constant of (“geometric strain effect”) Ru lead to a down-shift of the d -band center [24, 25], which reduces the binding strength of adsorbates on Pt layers on Ru(0001) in a cooperative fashion.

In all four cases shown in Fig. 3, the adsorption energy of H_{ad} in the middle of the Ru areas resembles that on extended Ru(0001) substrates. Looking at the situation close to the steps in more detail, we see that at the (111)-like step the first string of H adatoms on the Ru(0001) areas at the steps, on position 8 (square) in all four cases (Fig. 3a-d), is adsorbed with a binding energy in between that on Ru(0001) and on $\text{Pt}_{1\text{ML}}/\text{Ru}(0001)$ surfaces. In addition, also H_{ad} atoms on position 7 (square) are slightly less strongly bound than on the extended Ru(0001) surface. For adsorption on hcp sites (round symbols), where H_{ad} is generally slightly weaker bound by about 50 meV per atom and which are further away from this step edge, the modification is limited to the first string of atoms. On the other hand, for the other step edge with (100) sites, both the first (position 4, square) and the second (position 5, square) string of sites for the islands with four Pt rows (Fig. 3d) are (slightly) less strongly adsorbing than the Ru(0001) terraces. For adsorption on the hcp sites (round symbols), the modification is again limited to the first string of sites along the edge. Interestingly, at these steps adsorption on an on-top position (position 5, diamond) is somewhat stronger than adsorption on the neighbored hcp site (position 5, round symbol).

Similar considerations apply to the Pt islands. For the islands that are four atomic rows wide (Fig. 3d), the hydrogen adsorption energies in the middle of the island stripe, e.g., in positions 2 and 3 (square) are close to, but not fully at the optimum value obtained at the fcc site of an extended Pt/Ru(0001) overlayer system (see the dashed line in the panels in Fig. 3). Here it should be noted that on position 3 (square) the H_{ad} atom is slightly displaced from the fcc site, away from the step towards a neighboring bridge site. H_{ad} on the fcc site close to the opposite step (fcc facets) is unstable, and the atom relaxes towards a neighboring (111) step facet site. Adsorption on the hcp sites (round symbols), on the other hand, does not result in a (metastable) minimum, and the H_{ad} atoms relax to neighboring on-top sites instead, where adsorption is more stable than on both fcc and hcp on the Pt monolayer islands sites. This is demonstrated also by the weaker binding of H_{ad} atoms which were fixed on the hcp positions (positions 2 and 3, diamonds), and which yield binding energies comparable to those on the fcc sites. Interestingly enough, on the inner two rows of the four-atom wide Pt islands, the ordering in the adsorption site stability is the same as on Pt(111), namely with the top site being the most favorable adsorption site whereas on the Pt/Ru(0001) overlayer system the three-fold hollow site is the preferred hydrogen adsorption site, as on the underlying Ru(0001) substrate.

If the Pt islands are only three and less atomic rows wide (Fig. 3a-c), hydrogen binding is stronger on all sites than on the extended overlayer system. Thus both on the Pt islands as well as on the lower Ru terraces the influence of the steps extends over the first two atomic rows away from the step edges. Overall, these results demonstrate that also on the Pt monolayer island edge the steps result in a modification of the H_{ad} binding energy over more than just the nearest neighbor sites, i.e., also on the edge the step effects are longer-ranged. Considering both the upper and the lower terrace side of the steps and different step geometries, the presence of steps results in 3–4 sites per step atom with adsorption energies in between those of Ru(0001) and of the extended Pt monolayer, which can be occupied simultaneously, in good agreement with our experimental findings [12].

Comparing the hydrogen adsorption energies for the systems with Pt islands of three and four atomic Pt rows, we note that they are rather similar at the step edges and on the Ru terraces, although they are still different in the center of the Pt rows. Hence, Pt islands with three atomic rows are wide enough to lead to changes at the steps and the lower terrace that are characteristic for extended islands.

The above results can be rationalized by analyzing the underlying electronic structure of the metal atoms. In Fig. 4, the local Ru d -band centers are plotted for the four different Pt island sizes considered, the assignment of the Ru atoms corresponds to the one depicted in the upper panels of Fig. 3. Note that a larger coordination or a stronger interaction with the neighboring metal atoms leads to a down-shift of the local d -band. First of all it is obvious that the local d -band centers of the Ru atoms underneath the Pt atoms are lower than those on the Ru terrace. This can be explained by the larger coordination of these Ru atoms compared to the terrace atoms. Interestingly enough, the d -band center is lowest at the Ru atom closest to the (100)-like step edge. Obviously, the low coordination of the Pt step edge atom makes this Pt atom interacting more strongly with the underlying Ru atoms. The local Ru d -band centers of the atoms at the second

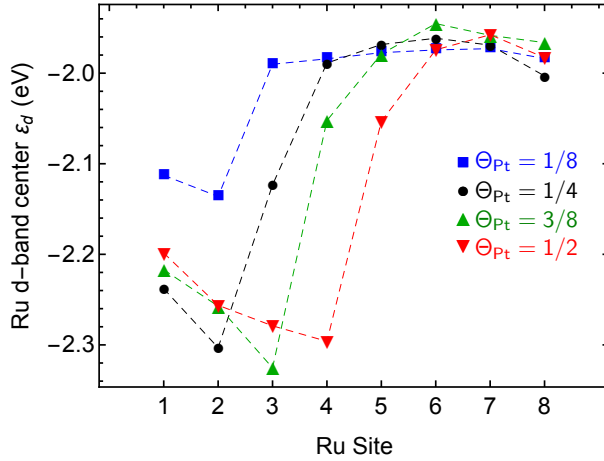


Fig. 4 Local Ru *d*-band centers of the Pt/Ru(0001) island systems. The Ru atoms are numbered according to the assignment given in the upper panels of Fig. 3.

rows away at the step edge are already rather close to the one in the middle of the lower terrace (for example, sites 5 and 8 for $\Theta_{\text{Pt}} = 3/8$).

Finally, we consider hydrogen adsorption on stepped Ru(10 $\bar{1}$ 9) without and with the steps decorated by one row of Pt atoms. Figure 5a, compares the adsorption energies on clean Ru(10 $\bar{1}$ 9) with those on flat Ru(0001). Note that the adsorption energies in the middle of the terraces (adsorption sites 1, 9 and 4, 5) are close to those on flat Ru(0001), whereas at the Ru steps the energy deviates considerably from the values on flat Ru(0001). There is a relatively strong deviation at the (111)-like edge (site 3) and a modest deviation at the (100)-like edge (site 7). Thus, like in the case of the Pt islands, the influence of the Ru steps extends over more than a single row of sites, in this case 1-2 rows, on either side of the step, depending on the step structure and on the type of adsorption sites considered.

In addition, we repeated the calculations, after replacing the Ru atoms at site 3 (Fig. 5b) or site 7 (Fig. 5c) by Pt atoms, which corresponds to decorating the steps by a row of Pt surface atoms. Note that metal steps decorated by one row of other metal atoms can be prepared experimentally with a high degree of control and are often used either to modify the chemical properties of the steps (see, e.g., [4]) or to create metallic wires with specific properties (see, e.g., [26]). First of all, the adsorption of H at the (100)-like edge is energetically more favored by 73 meV/H than at the (111)-like edge. The step decoration with Pt leads to lower hydrogen adsorption energies at the steps than on the pure Ru(10 $\bar{1}$ 9) surface. The influence of Pt is more pronounced on the upper terrace of the Pt row, sites 1 and 2 for Pt at the (111)-like edge and sites 5 and 6 for Pt at the (100)-like edge. On the lower terrace side, hydrogen adsorption is little affected compared to Ru(10 $\bar{1}$ 9) for Pt at the (111) like edge, while in the other case, Pt at the (100)-like edge, it is significantly weaker compared to adsorption at equivalent sites on the Pt-free stepped Ru(10 $\bar{1}$ 9) surface directly adjacent to the step (site

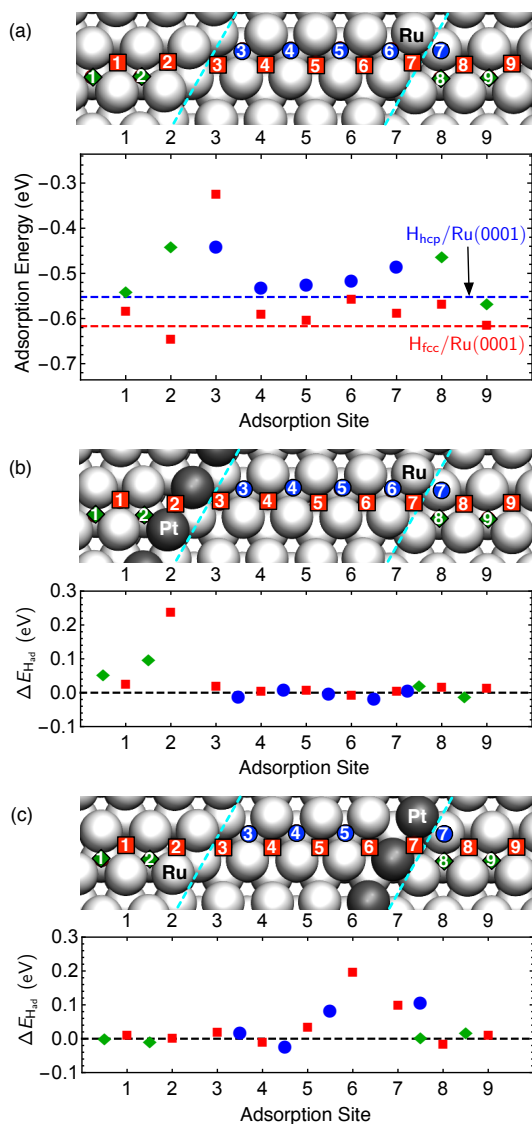


Fig. 5 Adsorption energy of isolated hydrogen atoms within a (1×2) geometry on clean Ru(101̄9) (panel a) and with the (111)-like step (panel b) and the (100)-like step (panel c) decorated with one atomic row of Pt. In panels b and c, the hydrogen adsorption energies ΔE are taken with respect to clean Ru(101̄9) (see dashed line). The dashed lines in panel a denote the hydrogen adsorption energies at the hcp and fcc sites of Ru(0001), respectively.

7 in Fig. 5c). Apparently, for larger distances, the additional modification by the step Pt decoration is too weak to be significant in the stepped surfaces.

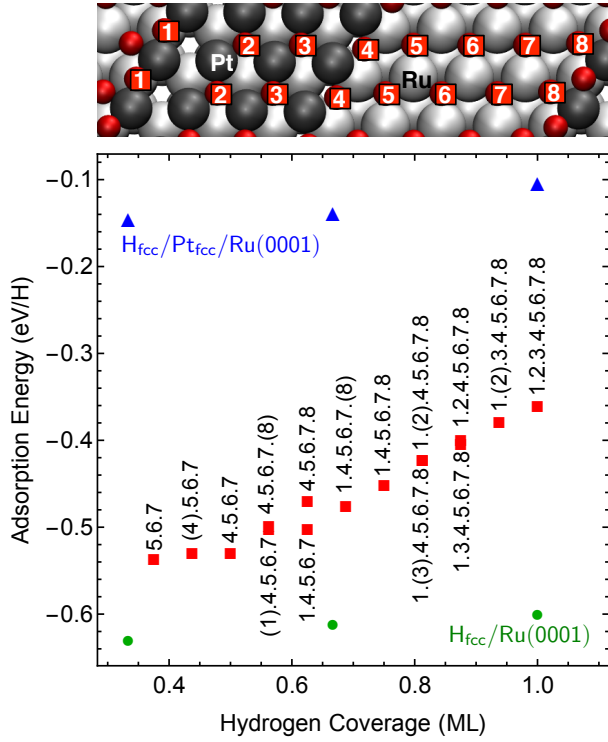


Fig. 6 Adsorption energy per hydrogen atom on Ru(0001) covered by a Pt island with $\Theta_{\text{Pt}} = 1/2$ as a function of hydrogen coverage. The labels in the figure denote the positions of the hydrogen atoms. The numbers in parentheses indicate that only one of the two equivalent sites in the (8×2) unit cell has been occupied. In addition, hydrogen adsorption energies on flat Ru(0001) and Pt/Ru(0001) at hydrogen coverages $\Theta_{\text{H}} = 1/3, 2/3$ and 1 are included.

3.3 Adsorption of hydrogen at higher coverages

In order to more realistically account for the situation during TPD experiments and also for comparison with electrochemical measurements, we studied hydrogen adsorption at higher coverages on Ru(0001) partially covered by Pt islands with $\Theta_{\text{Pt}} = 1/2$ whose structure is illustrated in the upper panel of Fig. 3d. We increased the coverage by first covering the Ru terraces which exhibit a stronger binding with respect to hydrogen than the Pt islands (see Fig. 3d). Successively, hydrogen atoms were added at the next most favorable adsorption site according to the adsorption energies for isolated hydrogen atoms, and these structures were then relaxed. The positions 1-8 shown in the upper panel of Fig. 6 do in fact correspond to the energy minimum configuration for the fully hydrogen-covered surface, but the single adsorption configurations hardly change as a function of coverage. On the Pt islands, no adsorption at the top sites occurs in spite of the fact that they are energetically favorable at low hydrogen coverage (see Fig. 3d). This is in fact analogous to hydrogen adsorption on Pt(111) [19]. Isolated hydrogen atoms prefer the top sites, but at higher coverages the three-fold hollow sites are energetically more favorable as the dipole-dipole repulsion between the adsorbed

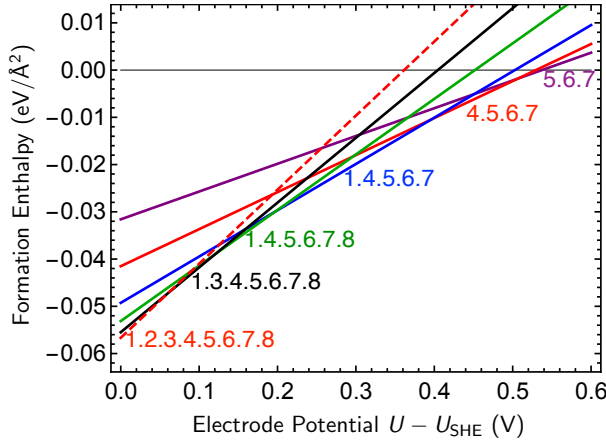


Fig. 7 Free energy of adsorption of hydrogen structures on Ru(0001) covered by a Pt island with $\Theta_{\text{Pt}} = 1/2$ as a function of the electrode potential determined based on the concept of the computational hydrogen electrode [29,30] assuming pH=0.

hydrogen atoms is reduced when the atoms are adsorbed closer to the first layer of metal atoms [27].

The mean adsorption energies per hydrogen atom calculated according to Eq. (1) are plotted as a function of the hydrogen coverage in Fig. 6. In addition, hydrogen adsorption energies on flat Ru(0001) and Pt/Ru(0001) at hydrogen coverages $\Theta_{\text{H}} = 1/3, 2/3$ and 1 are included. As mentioned above, first the lower Ru terrace becomes populated. Once adsorption on the Pt islands starts, the mean hydrogen adsorption energy becomes less negative, i.e., the average binding becomes weaker. Note that typically adsorbed hydrogen atoms exhibit a mutual repulsive interaction on close-packed metal surfaces [28,19]. However, the reduction energy due to the mutual repulsion is much weaker as the results for hydrogen adsorption on flat Ru(0001) and Pt/Ru(0001) included in Fig. 6 show. This demonstrates that the lowering of the mean adsorption energy as a function of coverage on partially Pt-covered Ru(0001) is mainly due to the weaker hydrogen binding on the Pt islands, once all Ru sites are populated.

Note that in Fig. 6 the average adsorption energy per hydrogen atom is plotted whereas in TPD experiments as shown in Fig. 2 rather differential adsorption energies, i.e., the energy gain upon adsorption of an additional hydrogen atom to a given structure, are probed. Of course, the differential adsorption energies can be deduced from the difference in the mean adsorption energies as a function of coverages. The approximately linear increase in the mean adsorption energies for coverage larger than 0.6 means that there is a range of differential adsorption energies once the Ru terraces are filled because for a jump to another constant differential adsorption energy the relative change would become smaller at higher coverage. This explains why there is a non-zero region in the TPD diagram between the two peaks associated with adsorption on the Ru substrate and on the extended Pt islands, respectively.

The evaluation of the hydrogen adsorption energies as a function of coverage also allows us to relate our findings to hydrogen deposition in an electrochemical

environment. Pt/Ru electrodes are often used as catalysts in the methanol electro-oxidation [31–34] in fuel cells. Furthermore, they also exhibit a favorable activity with respect to the oxygen reduction [35–38]. Using the concept of the computational hydrogen electrode [29], the stable hydrogen structures as a function of the electrode potential can be derived from the hydrogen adsorption energies on the Pt/Ru(0001) island (see Fig. 7). For details of this method, we refer to Ref. [39]. Note that in the explicit calculations, the effects arising from the presence of the electrolyte and the electrode potential are neglected. This simplification can be justified since water interacts relatively weakly with metal electrodes [40,41,30] and since the adsorption energies of oxygen, hydrogen and hydroxyl on metal electrodes hardly depend on an applied electric field [29,42]. The latter has been attributed to the small dipole moment associated with the adsorbed species [29], caused by the good screening properties of metals. Therefore, the hydrogen energies calculated for the metal-vacuum interface can still be used as a reasonable approximation to derive trends at the electrochemical metal-electrolyte interface.

As Fig. 7 shows, increasing the electrode potential leads to a sequence of stable hydrogen structures with decreasing hydrogen coverage. This is caused by the gradual change of the mean hydrogen adsorption energy as a function of coverage demonstrated in Fig. 6. According to DFT calculations, on Pt(111) as well as on Ru(0001), a hydrogen coverage of 1 is stable [34] which is higher than the experimentally determined maximum hydrogen coverage [43]. As the hydrogen adsorption on Ru is stronger, it is stable up to slightly higher potentials than on Pt(111). The presence of the Pt islands leads to a broader range of hydrogen adsorption energies, in particular as the hydrogen adsorption energy on the Pt islands is weaker than on Pt(111) [30], as discussed above. Thus the hydrogen desorption from the Pt/Ru(0001) island system starts at lower potentials than from Pt(111). These findings agree with cyclic voltammograms of Pt/Ru(0001) films [44] that confirm the weakening of the hydrogen bonding on Pt/Ru(0001) islands.

Finally, to further connect our results to electrochemical interfaces, we studied water monomer adsorption on the Pt/Ru islands with four atomic Pt rows. Just recently, we studied the adsorption of water monomers and ice-like hexagonal water layers on PtRu/Pt(111) surface alloys [45]. Single water molecules prefer to adsorb on the Ru sites of the PtRu surface alloy. Also the ice-like water layers tend to arrange in such a way as to maximize the water-Ru interaction.

The adsorption energies of isolated water molecules on Pt/Ru bimetallic surfaces with Pt islands consisting of four atomic rows are plotted in Fig. 8. We concentrated on the water adsorption energies at the steps and in the middle of the terraces. As for the PtRu/Pt(111) surface alloys, the water monomers also prefer the Ru sites on Ru(0001) with Pt monolayer islands; the water binding is stronger on the Ru terraces than on the Pt islands. Hence the water adsorption energies roughly follow the trends of the hydrogen adsorption energies shown in Fig. 3d. However, there is one different feature, namely the fact that water binds more strongly at sites 6 and 8 than at the terrace site 7. Apparently there is an additional attractive interaction of one hydrogen atom of the water molecule with the Pt step edge atom that stabilizes these particular adsorption geometries.

There is another difference between water and hydrogen adsorption. The water binding at the island edge site 4 in Fig. 8 is weaker than on site 2 close to the center of the islands. This is also surprising considering the fact that for example on

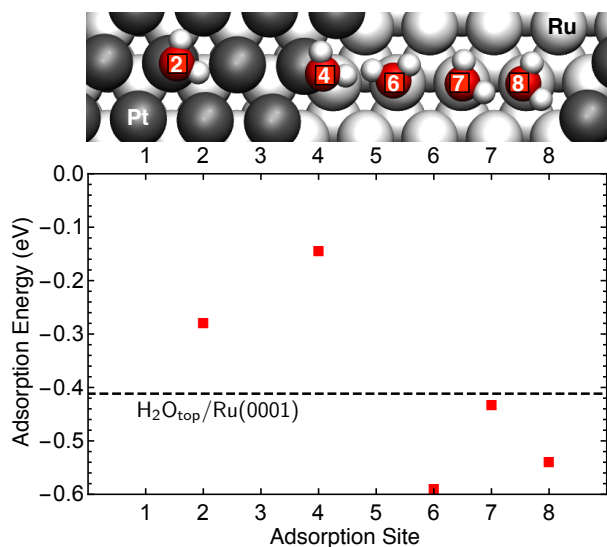


Fig. 8 Adsorption energy of isolated water molecules on Pt/Ru electrodes within a (8×2) geometry with Pt islands consisting of four atomic rows. The numbering of the atomic positions are illustrated in the panels above the diagrams. The dashed line denotes the water adsorption energies at the ontop site of Ru(0001). The energy minimum adsorption geometries of the isolated water molecules are shown in the upper panel.

Au(511) the water molecules bind much stronger on the low-coordinated step edge sites than on the terrace sites [46,47]. As Fig. 8 shows, at the island edge site the water molecule is drawn towards the Ru terraces, so that a tilted water adsorption geometry results. Apparently, the non-bonding interaction of the hydrogen atom with the Ru terrace reduces the binding strength.

4 Conclusions

Based on first-principles calculations, hydrogen adsorption energies on Pt monolayer island modified Ru(0001) and on stepped Ru surfaces decorated by an atomic Pt row were derived. On these bimetallic Pt/Ru surfaces, hydrogen adsorbs preferentially at the Ru sites, while the Pt sites interact less strongly with hydrogen than pure Pt(111) due to a combination of electronic ligand and the geometrical strain effects. The calculations show that the influence of the island edges and steps is not restricted to the nearest neighbor sites along the island edges, thus confirming the results of recent experimental observations. The results can be rationalized by the change of the electronic structure of the surface atoms, which is not restricted to the immediate vicinity of island edges and electrode steps. Water adsorption on a Pt/Ru island system exhibits similar trends, however, the binding is modified due to the additional interaction of the hydrogen atoms of the water molecule with the island edges.

Acknowledgments

This research has been supported by the German Research Foundation (DFG) through contract GR 1503/22-2 and BE 1201/18-2 within the DFG Research Unit FOR 1376. Computer time has been provided by the state of Baden-Württemberg through the bwHPC project and the Germany Research Foundation (DFG) through grant number INST 40/467-1 FUGG.

References

1. K. Christmann, G. Ertl, Surf. Sci. **60**, 365 (1976). DOI [http://dx.doi.org/10.1016/0039-6028\(76\)90322-8](http://dx.doi.org/10.1016/0039-6028(76)90322-8)
2. B. Poelsema, G. Mechttersheimer, G. Comsa, Surf. Sci. **111**, 519 (1981). DOI [http://dx.doi.org/10.1016/0039-6028\(81\)90406-4](http://dx.doi.org/10.1016/0039-6028(81)90406-4)
3. B. Hammer, O.H. Nielsen, J.K. Nørskov, Catal. Lett. **46**, 31 (1997)
4. P. Gambardella, Ž. Šljivančanin, B. Hammer, M. Blanc, K. Kuhnke, K. Kern, Phys. Rev. Lett. **87**, 056103 (2001)
5. A. Groß, J. Comput. Theor. Nanosci. **5**, 894 (2008)
6. B. Hammer, J.K. Nørskov, Surf. Sci. **343**, 211 (1995)
7. H.S. Taylor, Proc. R. Soc. Lond. A **108**, 105 (1925). DOI 10.1098/rspa.1925.0061
8. S. Dahl, A. Logadottir, R.C. Egeberg, J.H. Larsen, I. Chorkendorff, E. Törnqvist, J.K. Nørskov, Phys. Rev. Lett. **83**, 1814 (1999)
9. L. Jacobse, A. den Dunnen, L.B.F. Juurlink, J. Chem. Phys. **143**, 014703 (2015). DOI <http://dx.doi.org/10.1063/1.4923006>
10. C. Badan, R.G. Farber, Y. Heyrich, M.T.M. Koper, D.R. Killelea, L.B.F. Juurlink, J. Phys. Chem. C **120**, 22927 (2016). DOI 10.1021/acs.jpcc.6b05482
11. A.M. Gómez-Marín, J.M. Feliu, Catal. Today **244**, 172 (2015). DOI <http://dx.doi.org/10.1016/j.cattod.2014.05.009>
12. H. Hartmann, T. Diemant, J. Bansmann, R.J. Behm, Phys. Chem. Chem. Phys. **14**, 10919 (2012). DOI 10.1039/C2CP41434A
13. M.F. Juárez, E. Santos, J. Phys. Chem. C **117**(9), 4606 (2013). DOI 10.1021/jp311531u
14. M.F. Juárez, E. Santos, J. Phys. Chem. C **120**, 2109 (2016). DOI 10.1021/acs.jpcc.5b08041
15. A. Ruderman, M. Juarez, L. A. Valle, G. Beltramo, M. Giesen, E. Santos, Electrochem. Commun. **34**, 235 (2013). DOI <http://dx.doi.org/10.1016/j.elecom.2013.06.023>
16. G. Kresse, J. Furthmüller, Phys. Rev. B **54**, 11169 (1996)
17. P.E. Blöchl, Phys. Rev. B **50**, 17953 (1994)
18. J.P. Perdew, K. Burke, M. Ernzerhof, Phys. Rev. Lett. **77**, 3865 (1996)
19. S. Schnur, A. Groß, Catal. Today **165**, 129 (2011). DOI doi: 10.1016/j.cattod.2010.11.071
20. A. Groß, Topics Catal. **37**, 29 (2006)
21. J. Greeley, J.K. Nørskov, L.A. Kibler, A.M. El-Aziz, D.M. Kolb, Chem. Phys. Chem. **7**, 1032 (2006)
22. S. Sakong, C. Mosch, A. Groß, Phys. Chem. Chem. Phys. **9**, 2216 (2007)
23. A. Groß, J. Phys.: Condens. Matter **21**, 084205 (2009)
24. A. Schlapka, M. Lischka, A. Groß, U. Käsberger, P. Jakob, Phys. Rev. Lett. **91**, 016101 (2003)
25. M. Lischka, C. Mosch, A. Groß, Electrochim. Acta **52**, 2219 (2007). DOI 10.1016/j.electacta.2006.03.113
26. P. Gambardella, M. Blanc, H. Brune, K. Kuhnke, K. Kern, Phys. Rev. B **61**, 2254 (2000). DOI 10.1103/PhysRevB.61.2254
27. A. Groß, *Theoretical surface science – A microscopic perspective*, 2nd edn. (Springer, Berlin, 2009)
28. A. Roudgar, A. Groß, J. Electroanal. Chem. **548**, 121 (2003)
29. J.K. Nørskov, J. Rossmeisl, A. Logadottir, L. Lindqvist, J.R. Kitchin, T. Bligaard, H. Jónsson, J. Phys. Chem. B **108**, 17886 (2004). DOI 10.1021/jp047349j
30. S. Sakong, M. Naderian, K. Mathew, R.G. Hennig, A. Groß, J. Chem. Phys. **142**, 234107 (2015). DOI <http://dx.doi.org/10.1063/1.4922615>
31. H.A. Gasteiger, N. Marković, P.N. Ross, E.J. Cairns, J. Electrochem. Soc. **141**, 1795 (1994). DOI 10.1149/1.2055007

32. H.E. Hoster, T. Iwasita, Baumgärtner, W. Vielstich, *Phys. Chem. Chem. Phys.* **3**, 337 (2001)
33. R. Reichert, J. Schnaidt, Z. Jusys, R.J. Behm, *Phys. Chem. Chem. Phys.* **16**, 13780 (2014). DOI 10.1039/C4CP01229A
34. S. Sakong, A. Groß, *ACS Catal.* **6**, 5575 (2016). DOI 10.1021/acscatal.6b00931
35. J.L. Zhang, M.B. Vukmirovic, Y. Xu, M. Mavrikakis, R.R. Adzic, *Angew. Chem. Int. Ed.* **44**, 2132 (2005)
36. R.A. Sidik, A.B. Anderson, *J. Electroanal. Chem.* **528**, 69 (2002)
37. J.X. Wang, N.M. Marković, R.R. Adžić, *J. Phys. Chem. B* **108**, 4127 (2004)
38. S. Brimaud, A.K. Engstfeld, O.B. Alves, H.E. Hoster, R.J. Behm, *Top. Catal.* **57**, 222 (2014). DOI 10.1007/s11244-013-0177-0
39. F. Gossenberger, T. Roman, A. Groß, *Electrochim. Acta* **216**, 152 (2016). DOI <http://dx.doi.org/10.1016/j.electacta.2016.08.117>
40. A. Roudgar, A. Groß, *Chem. Phys. Lett.* **409**, 157 (2005)
41. A. Roudgar, A. Groß, *Surf. Sci.* **597**, 42 (2005)
42. J. Rossmeisl, J.K. Nørskov, C.D. Taylor, M.J. Janik, M. Neurock, *J. Phys. Chem. B* **110**, 21833 (2006). DOI 10.1021/jp0631735
43. N.M. Marković, P.N. Ross Jr., *Surf. Sci. Rep.* **45**, 117 (2002)
44. H.E. Hoster, O.B. Alves, M.T.M. Koper, *ChemPhysChem* **11**, 1518 (2010). DOI 10.1002/cphc.200900500
45. J.M. Fischer, D. Mahlberg, T. Roman, A. Groß, *Proc. R. Soc. A* **472**, 20160618 (2016). DOI 10.1098/rspa.2016.0618
46. X. Lin, A. Groß, *Surf. Sci.* **606**, 886 (2012)
47. A. Groß, F. Gossenberger, X. Lin, M. Naderian, S. Sakong, T. Roman, *J. Electrochem. Soc.* **161**, E3015 (2014). DOI 10.1149/2.003408jes